Proc. 5th Australian Wind Engineering Conf. Adelaide, Feb.1996

DYNAMIC RESPONSE OF 1:12 SCALE CAR MODEL WITH DIFFERENT REAR-END MODIFICATIONS IN TURBULENT WINDS

T. M. Nguyen, J.W. Saunders, S. Watkins
Royal Melbourne Institute of Technology

1. Introduction

In recent years, lighter materials and more streamlined designs have been applied to road vehicles to save energy and increase performance. However road vehicles are generally less aerodynamically stable because the centre of pressure on the vehicles is tending to move forward with reducing drag coefficients.

To investigate the dynamic response of passenger cars, an experiment was undertaken with a car model based on a shape proposed by the Society of Automotive Engineers (1990) at the Royal Melbourne Institute of Technology Wind Tunnel to measure the dynamic response of the car with different rear-end shapes (sedan, fast back, hatch back and station wagon) in a range of yaw angles from 0 to 40° in grid-generated turbulent wind. Side forces and longitudinal velocities were recorded and then analysed in applying the concept of aerodynamic admittance for side force. Initial results suggested a good agreement with Cooper's theory (1984). A new approach is suggested using "force intensity" for consideration to the aerodynamic admittance for side force.

3. Theoretical background

The aerodynamic admittance is defined as the transfer function between fluctuating wind velocity and fluctuating force applied to the vehicle. After Davenport (1961) and then Cooper (1984) the side force aerodynamic admittance is defined as

$$|X(n)|^2 = \frac{1}{4}\frac{\Phi_s(n)}{\bar{S}^2} / \frac{\Phi_u(n)}{\bar{U}^2} \qquad (1)$$

where $\Phi_u(n)$ and $\Phi_s(n)$ are spectra of longitudinal wind velocity and side force, $\bar{U}$ and $\bar{S}$ are mean values of longitudinal wind velocity and side force.

For most engineering purposes, when the vehicle speed is higher than two times the atmospheric wind speed, Cooper proposed an approximation of the aerodynamic admittance as

$$|X(n)|^2 = \frac{1}{1+\left[2.5(nL_x/V_R)(L/L_x)\right]^3} \qquad (2)$$

where n is frequency, L is car length, L_x is turbulence length scale of longitudinal velocity and V_R is the relative wind speed with reference to moving vehicle.

Cooper's assumption is reasonable because for most driving conditions, the car speed would be from 90-100 km/h (25-28 m/s) and the atmospheric wind speed is less than 10 m/s [Watkins et al (1995)].

Note that equation (1) can be rewritten as :

$$|X(n)|^2 = \frac{1}{4}\frac{n\Phi_s(n)/\sigma_s^2}{n\Phi_u(n)/\sigma_u^2}\frac{I_s^2}{I_u^2} \qquad (3)$$

where

- $I_u = \sigma_u / \bar{U}$ is the longitudinal turbulence intensity
- σ_u is the standard deviation of fluctuating u-component of wind velocity,
- σ_s is the standard deviation of fluctuating side force.
- $I_s = \sigma_s / \bar{S}$ is called **"force intensity"**

The order of $n\Phi_s(n)/\sigma_s^2$ and $n\Phi_u(n)/\sigma_u^2$ would be similar because: $\sigma^2 = \int_0^\infty \Phi(n)dn$ (4)

therefore the ratio I_s^2/I_u^2 could be expected to determine the magnitude of side force aerodynamic admittance.

4. Experimental arrangement and procedure

The experiments were conducted in the RMIT wind tunnel with a 2 m x 3 m by 9 m long working section. The tunnel is of the closed-return type and has a free-stream turbulence intensity of 1.7 % and a top speed of 40 m/s. A highly turbulent flow was generated by the installation of a square-mesh grid at the inlet to the wind tunnel contraction. The grid had a bar size of 18cm and a spacing of also 18cm. Turbulence measurements were made with un-linearised single TSI constant-temperature hot-wire anemometers at the centre of the wind tunnel turntable and the distance from the grid was 3.7m (> 20 times mesh size). The characteristics of the turbulence will be described in the next section.

A 1:12 scale car model was mounted on a force balance bolted to the tunnel turntable. Different rear-end modifications to simulate fast back, hatch back and station wagon were added during the experiments.

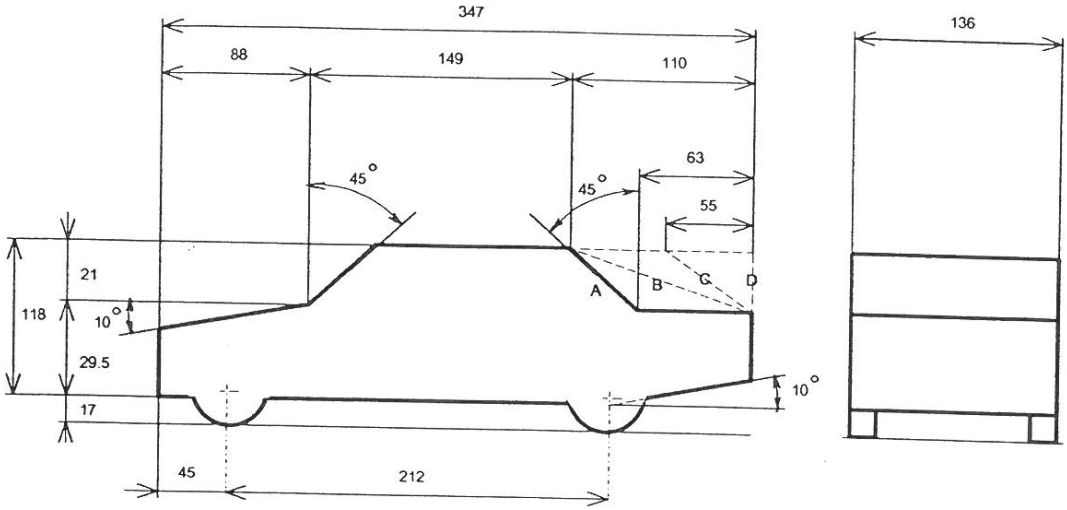

Figure 1. Basic model with four alternative rear end shapes A, B, C, D corresponding to sedan, fast back, hatch back and station wagon

Mean and fluctuating forces were sensed by a semi-conductor strain-gauged force balance. The lowest natural frequency n_o of the whole system including the model was about 115 Hz and the damping ratio ζ of the system was found to be 0.02.

Longitudinal velocity and force signals were recorded on a Sony DAT PC116 tape recorder. These signals were then later digitised on a PC with a Data Translation analogue-to-digital board DT2814.

5. Experimental results

5.1 Flow characteristics

With the grid in position, the longitudinal turbulence intensity increased to 13.5 %. The velocity and turbulence intensity profiles were essentially constant in the vertical and lateral direction with no significant variation. The turbulence length scale of the u-component of velocity was found to be 0.125m - equivalent to 1.5m in full scale and calculated from the formula

$$L_x = \int_0^\infty R(\tau)d\tau \qquad (5)$$

where $R(\tau)$ is the auto-correlation function of u-component at time lag τ.

The turbulence scale was substantially lower than the on-road conditions. However Melbourne (1979) and Akins (1989) argue that for bluff body flows it is important to simulate the high frequency portion of the spectra rather than the low frequency portion. The turbulence intensity in the experiments may be considered as high, relative to the typical values experienced by on-road cars of 3-5% [Watkins et al (1995)].

Figure 2 represents the spectrum of longitudinal wind velocity versus reduced frequency $2\pi L_x / \overline{U}$ and compared with Von Karman wind spectrum model.

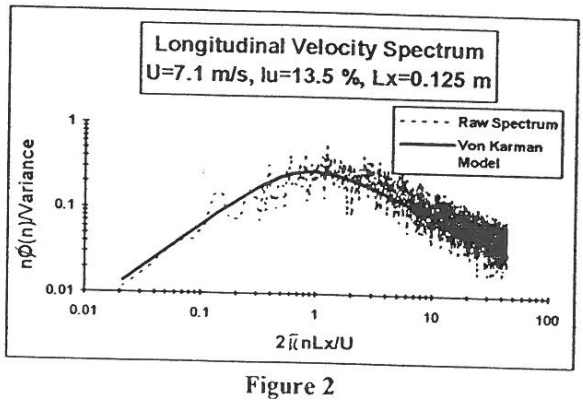

Figure 2

With the variation of wind tunnel speed, the turbulence intensity and turbulence scale at the test position were found to be almost constant (See Figure 3).

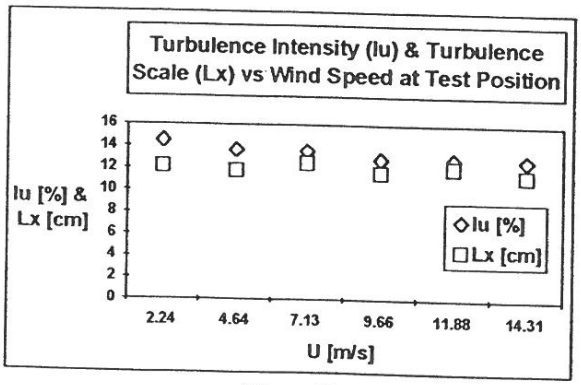

Figure 3

5.2 Reynolds number checks

Before proceeding with experiments, Reynolds number checks were carried out. Figure 4 represents the

variation of mean and unsteady side force coefficients with Reynolds number for sedan shape at 15° yaw angle. These coefficients are defined as:

- Steady side force coefficient:

$$C_s = \bar{S} / (1/2 \rho \bar{U}^2 A)$$

- Unsteady side force coefficient:

$$C_s' = \sigma_s / (1/2 \rho \bar{U}^2 A)$$

where ρ is air density and A is the model frontal area.

The Reynolds number is defined as : $Re = \bar{U}D / \nu$

where D is the car width and ν is the kinematic viscosity of air. It can be seen from these figures that Reynolds number effects are small, especially at the high wind tunnel speeds.

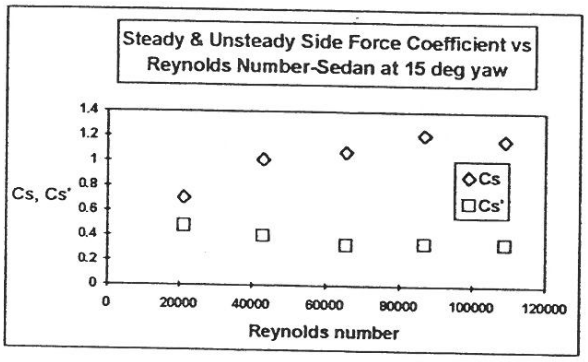

Figure 4

5.3 Steady side force measurements

Figure 5 shows the variation of steady side force coefficients for different car shapes versus yaw angles from 0 to 40°. It could be seen that mean side force increases with yaw angle and also with the side area respectively from sedan to fast back, hatch back and station wagon

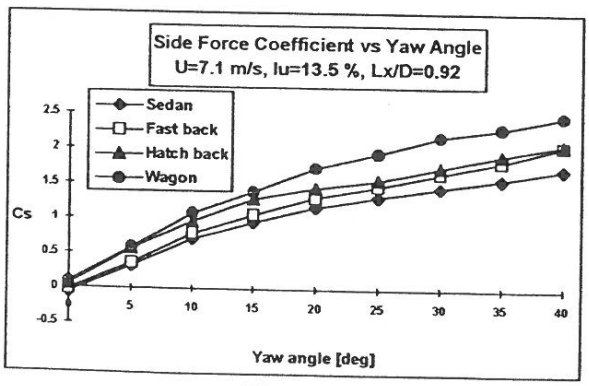

Figure 5

5.4 Unsteady side force measurements

Figure 6 represents the variation of unsteady side force coefficients for different car shapes versus yaw angles. It is noticeable that the unsteady side force was also significant at low yaw angles and it increases with side area. As expected, the station wagon shape vibrates more than hatch back, fast back and sedan shape respectively.

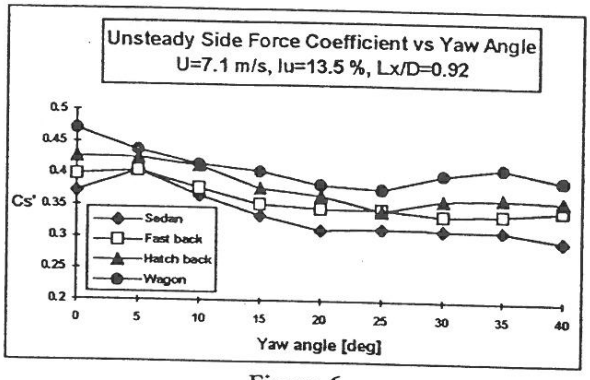

Figure 6

If the unsteady side force is divided by the steady side force coefficient, the result would represent a quantitative value of side force vibration similar to the turbulence intensity, which has been defined here as the concept of "force intensity" (I_s). It is noticeable that force intensity varies in an inversing order with yaw angles (See Figure 7).

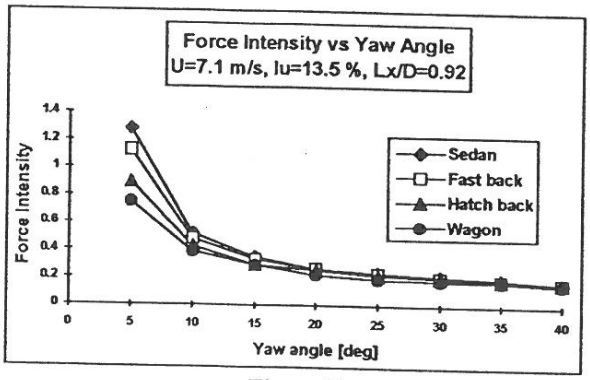

Figure 7

Side force spectra were calculated and displayed in dimensionless form of $n\Phi_s(n)/\sigma_s^2$ against Strouhal number $nD/\bar{U}$. From Figures 8 and 9, it could be seen that dimensionless side force spectra for various yaw angles and rear-end shapes were very similar and all have a peak at a Strouhal number of about 0.1. The yaw angles have been chosen as 10, 20, 30, 40° for a sedan shape and in comparing effect of shape, the yaw angle chosen was 30°.

Because the wind velocity spectrum and turbulence intensity in all cases is similar as well as side force spectra, the force intensity may be the parameter affecting the magnitude of aerodynamic admittance.

The side force aerodynamic admittance for the shapes tested were calculated from equation (3). For a typical 30^0 yaw angle, the aerodynamic admittances were

plotted in the Figure 10 including Cooper's theoretical values.

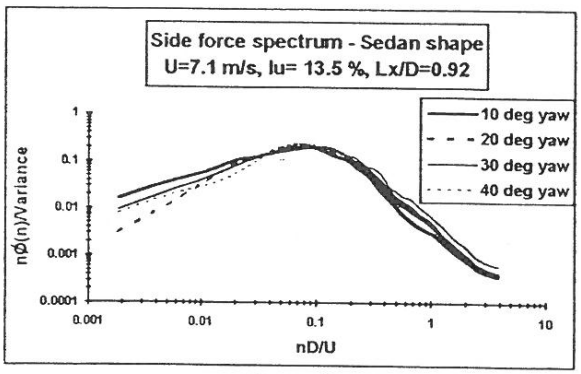

Figure 8

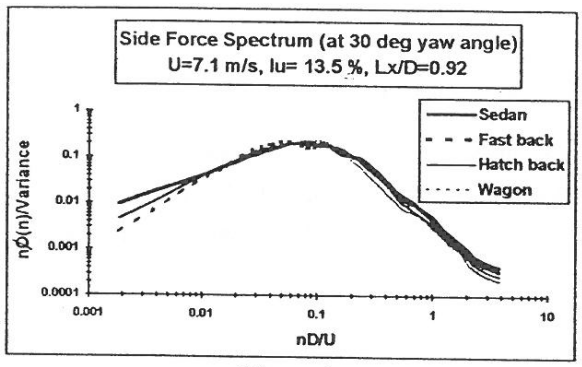

Figure 9

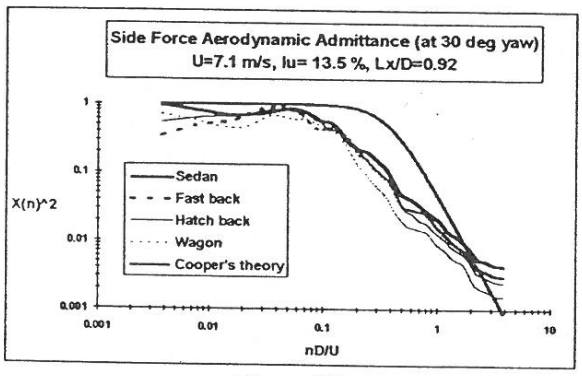

Figure 10

6. Concluding remarks

From the initial experimental results on sharp-edged model cars, the following points are made :

- The investigation on the dynamic response of passenger cars in turbulent crosswinds may be concentrated on a basic shape - for example a sedan and the results were found to vary little between sedan, fast back, hatch back and station wagon.
- It appears possible to generalise the side force spectrum as a curve with the peak at a reduced frequency of 0.1. However this needs to be further investigated in different flows before introducing an empirical formula for side force spectra.
- The experimental values of aerodynamic admittance agree quite well with Cooper's theory at large yaw angles. In the range of reduced frequencies between 0.1 to 1 the experimental aerodynamic admittance was lower than predicted by Cooper.
- The concept of "force intensity" may be useful in considering the aerodynamic admittance.
- In order to improve the experimental work, a very stiff balance would be an improvement for dynamic measurements to avoid dynamic calibration and correction. A flow visualisation would also be useful to understand the effects of model shape and turbulence.

In conclusion, the experiments could prove the application of Cooper's theory of side force aerodynamic admittance to passenger cars. However the scope of the study should be extended to include yawing and rolling moments and to improve the turbulence simulation. The introduction of the concept of "force intensity" may suggest an approach to understand the crosswind stability of road vehicles.

7. Acknowledgments:

The authors would like to thank the Commonwealth Government, RMIT Mechanical Engineering Department, Monash University and A.Prof. L. Peterson for his comments.

8. References

- Aerodynamic Testing of road vehicles - J2071 Mar90, SAE information report.
- C.J. Baker, The behaviour ofroad vehicles in unsteady cross winds, J. Wind Eng. Ind. Aerodyn. 49 (1993) 439-448.
- P.W. Bearman, 1969, Nat. Phys. Lab. Aero. Rep. no. 1296.
- P.W. Bearman. Effect of free stream turbulence on the flow around bluff bodies, Prog. Aerospace Sci. Vol 20, pp. 97-123, 1983
- P.W. Bearman and S.P. Mullarkey, Aerodynamic forces on road vehicles due to steady side winds and gusts, Proc. Royal Aeronautical Society, 18-19/7/1994
- S.A. Coleman, C.J. Baker, An experimental study of the aerodynamic behaviour of high sided lorries in cross winds, J. Wind Eng. Ind. Aerodyn. 53 (1994) 401-429
- R.K. Cooper, Atmospheric turbulence with respect to moving ground vehicles, J. Wind Eng. Ind. Aerodyn. 17(2) (1984) 215-238.
- A.G. Davenport, The application of statistical concepts to the wind loading of structures, Proc. Inst. Civil Eng 1961, Vol 19, 449-472.11
- W.H. Melbourne, Turbulence effects on maximum surface pressures - a mechanism and possibility of reduction, Proc. 5th Int. Conf. on Wind Engineering, Fort Collins, 1979, pp. 541-551.
- H.W. Tielman and R.E. Akins, Effect of incident turbulence on the pressure distribution on rectangular cylinders, Proc. 6th US Wind Engineering Conf., Houston, 1989, Paper B4 1-10.
- B.J. Vickery (1968). Wind load on buildings. PhD Thesis
- S. Watkins and J.W. Saunders, Turbulence experienced by road vehicles under normal driving conditions, Int. Cong. and Expos., Detroit, Michigan, Feb 27- Mar 2, 1995, SAE950997